DOI: 10.1002/ejoc.200701066

Stable-Ion NMR and GIAO-DFT Study of the Carbocations from Benzofluorenes and Dibenzofluorenes; Synthesis of Nitro Derivatives; Mutagenicity Assay and X-ray Analysis

Kenneth K. Laali,*[a] Takao Okazaki,[a] Fatima Sultana,[a] Scott D. Bunge,[a] Bimal K. Banik,[b] and Carol Swartz[c]

Keywords: Carbocations / Benzo- and Dibenzofluorenes / Nitro derivatives / Mutagenicity / NMR and DFT

First examples of stable carbocations are reported from 7*H*-benzo[*c*]fluorene (**2**), 11*H*-benzo[*b*]fluorene (**3**), 11*H*-benzo[*a*]fluorene (**4**), 2-methoxy- (**5**), 7-methoxy- (**6**), and 9-methoxy-11*H*-benzo[*a*]fluorene (**7**), 7*H*-dibenzo[*c*,*g*]fluorene (**8**), 13*H*-dibenzo[*a*,*g*]fluorene (**9**), 2-methoxy-13*H*-dibenzo[*a*,*g*]-fluorene (**10**) and 5,6-dihydro-13*H*-dibenzo[*a*,*g*]fluorene (**11**). Charge-delocalization modes in the resulting carbocations were derived based on experimental and/or computed (GIAO-DFT) $\Delta\delta^{13}$C values and through the NPA-derived changes in charges (Δq). Whereas protonation regioselectivity in the parent systems (**2**, **3**, **4**, **8**, and **9**) corresponds to the energetically most favored carbocations computed by DFT, selectivity in the OMe-substituted derivatives (**5**, **6**, **7**, **10**, and **11**) is strongly controlled by the methoxy group. Benzofluorenes **3**, **5**, **6**, and **7** and dibenzofluorenes **8**, and **10** were nitrated under very mild conditions. Nitration selectivity in the parent systems **3** and **8** parallels those in stable-ion protonation, whereas regioselectivity in the MeO derivatives (**6**, **7**, and **10**) corresponds more closely to relative arenium ion energies in the parent unsubstituted systems. Comparative mutagenicity assays (Ames tests) were performed on **3NO$_2$**, **5NO$_2$**, **7NO$_2$**, **8NO$_2$**, and **10NO$_2$** relative to their precursors. Compounds **10NO$_2$**, **7NO$_2$**, and **8NO$_2$** were found to be potent direct-acting mutagens (with **10NO$_2$**, **8NO$_2$** also capable of acting as potent indirect mutagens). The X-ray structures of **5NO$_2$** and **8NO$_2$** were determined. The angle between the plane of the nitro group and the aromatic ring bearing the NO$_2$ group is 89.4° in **5NO$_2$** and 32.4° in **8NO$_2$**.

Introduction

Parent fluorene (**1**) constitutes a core structure for a relatively large class of *nonalternant* PAHs that are derived from mono- and dibenzannulation to **1** by various annulation modes, resulting in the formation of isomeric benzofluorenes and dibenzofluorenes (see Figure 1).

7*H*-Benzo[*c*]fluorene (**2**) is a component of coal tar. It forms DNA adducts in lung and was shown to be responsible for causing lung tumors in animal tests.[1,2] The *trans*-dihydrodiol and the *anti*- and *syn*-diol epoxide of **2**, in which the epoxide occupies a pseudo-bay region, were synthesized by Harvey et al.[3] as probable active metabolites of **2**. The dibenzofluorenes **8** and **9** can be viewed as the *nonalternant* analogs of benzo[*c*]phenanthrene and dibenzo[*a*,*h*]anthracene, respectively. Banik et al.[4] developed a one-pot alkylation and cyclodehydration method for the synthesis of **9**, and this opened up the possibility for the synthesis of substituted derivatives.[5] Derivatives of **9** have been shown to exhibit antitumor activity.[5] Nitration and bromination of **2** was reported to take place at C-5.[6a] Formylation of **3** was reported to give the 5-carbaldehyde,[6b] and bromination of **8** gave the 5-bromo derivative.[6c,6d] The electrophilic chemistry of **4** has apparently not been studied.[7a] Nitration and sulfonation of **9** were reported in the old literature, without establishing the position of substitution.[7b] Nitration of **9** with Bi(NO$_3$)$_3$[8a] and HNO$_3$[8b,8c] gave the 5-nitro derivative, and acetylation of **9** with acetic anhydride and AlCl$_3$ afforded the 5-acetyl derivative.[8c]

Nitrofluorenes (NFs) are produced in the environment by combustion of fossil fuel and have been shown to be mutagenic and carcinogenic.[9] It was shown that 2,7-DNF forms DNA adducts primarily by nitro reduction (nitro → nitroso → hydroxylamine), with the major adduct identified as 2-amino-*N*-(deoxyguanosin-8-yl)-7-NF.[9] To the best of our knowledge, biological activity of the nitro derivatives of benzofluorenes and dibenzofluorenes have not been studied.

Availability of the benzofluorenes **2**–**7**, dibenzofluorenes **8** and **9**, and their derivatives **10** and **11** (Figure 1) made possible the present combined stable-ion and nitration

[a] Department of Chemistry, Kent State University, Kent, OH 44242, USA
Fax: +1-330-6723816
E-mail: klaali@kent.edu
[b] Department of Chemistry, The University of Texas-Pan American, Edinburg, TX 78539, USA
[c] Environmental Carcinogenesis Division, US Environmental Protection Agency, Research Triangle Park, NC 27711, USA
Supporting information for this article is available on the WWW under http://www.eurjoc.org/ or from the author.

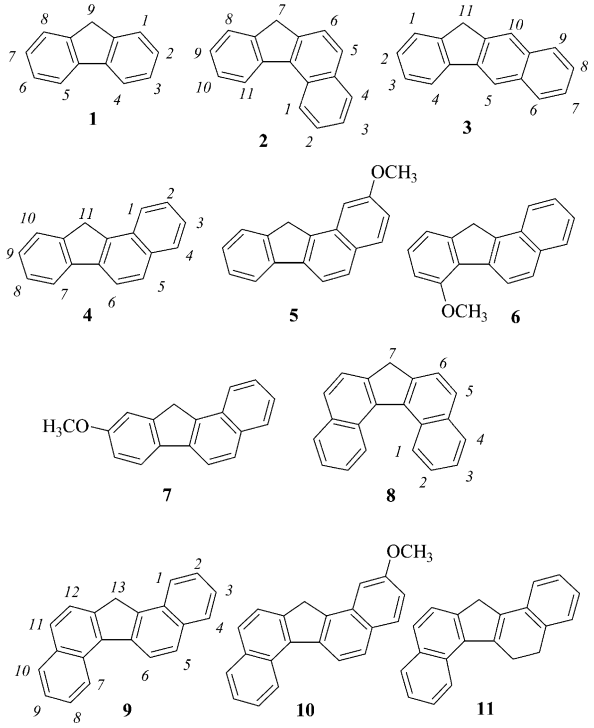

Figure 1. Studied benzofluorenes, dibenzofluorenes, and dihydrodibenzofluorene.

study. Moreover, synthesis and isolation of the nitro derivatives described herein opened up the possibility to examine their biological activity by comparative mutagenicity assay, and to explore their structures by X-ray analysis.

Results and Discussion

Ma and Johnson[10] reported the formation of the parent fluorenium cation (C-2-protonated) in $[Me_3S][Br]/AlBr_3/HBr$ (only ^1H NMR spectroscopic data were reported). The present study focuses on the benzannulated derivatives **2**–**11**, from which stable carbocations were generated in FSO_3H/SO_2ClF and in some cases in FSO_3H/SbF_5 (4:1)/SO_2ClF, for complete NMR characterization. Complete NMR spectroscopic data for the neutral PAHs are gathered in Figure S1. Specific NMR assignments were assisted by various 2D and 1D techniques (HMQC, HMBC, COSY, and NOE).

Stable-Ion Study of the Parent Benzofluorenes 2–4 and Dibenzofluorenes 8–9

See Scheme 1, Figures 2 and 3, and Table S1. Low-temperature reaction of 7*H*-benzo[*c*]fluorene (**2**) with FSO_3H/SO_2ClF gave $\mathbf{2H^+}$ as the sole carbocation by protonation at C-5. This outcome is in concert with DFT, from which the following sequence of relative carbocation stability was derived: C-5 > C-9 > C-11. The signals of the pseudo-fjord protons (1-H/11-H) in $\mathbf{2H^+}$ are at δ = 9.21 and 9.01 ppm, respectively, and exhibit mutual NOEs. Experimental and GIAO-derived NMR spectroscopic data for $\mathbf{2H^+}$ are gathered in Figure 2 for comparison. The positive charge is extensively delocalized throughout the periphery. The same charge-delocalization pattern was derived based on the computed changes in charges (Δq).

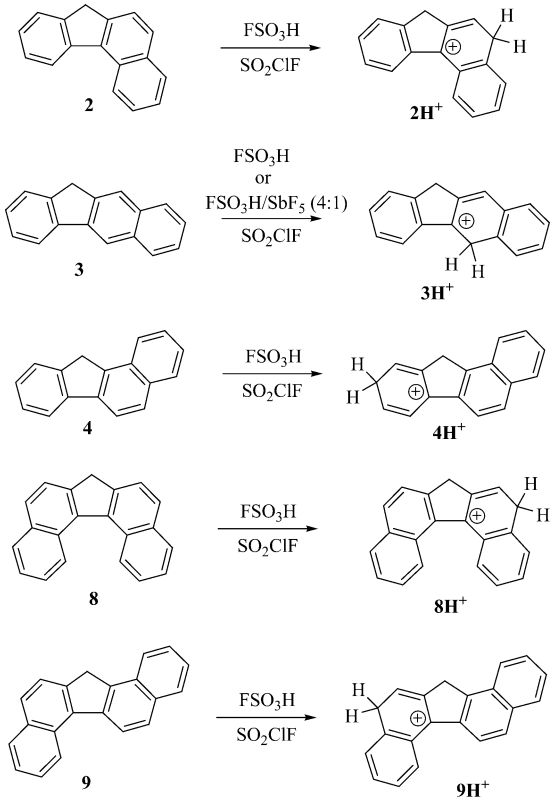

Scheme 1. Stable-ion study of parent benzofluorenes **2**–**4** and dibenzofluorenes **8** and **9**.

The following sequence of relative carbocation stability was derived by DFT for the protonation of 11*H*-benzo[*b*]fluorene (**3**): C-5 > C-6 > C-8 ≈ C-2. In agreement with this, low-temperature reaction of **3** with FSO_3H/SO_2ClF or with FSO_3H/SbF_5 (4:1)/SO_2ClF resulted in the formation of $\mathbf{3H^+}$ as the sole carbocation by protonation at C-5. Experimental and GIAO-derived charge-delocalization maps as well as the computed Δq map for $\mathbf{3H^+}$ indicate extensive charge delocalization with a very similar overall pattern as that in $\mathbf{2H^+}$.

Low-temperature reaction of 11*H*-benzo[*a*]fluorene (**4**) with FSO_3H/SO_2ClF led to the formation of $\mathbf{4H^+}$ by protonation at C-9. This agrees with the DFT-derived relative carbocation stability order C-9 > C-1 > C-3 = C-7 (Table S1 in Supporting Information). In this case, the arenium ion of protonation at C-1 (the naphthalene moiety) lies just 1 kcal/mol higher in energy. The experimental and GIAO-derived $\Delta\delta^{13}C$ values and the computed Δq map are sketched in Figure 2. The positive charge in $\mathbf{4H^+}$ is relatively less dispersed and resides mainly within the fluorene moiety.

Protonation at C-5 is computed by DFT to be the clear choice for 7*H*-dibenzo[*c*,*g*]fluorene (**8**), for which the relative stability order C-5 >> C-4 > C-2 was computed (Table S1). In concert with this, the low-temperature reaction of **8** with FSO_3H/SO_2ClF led to $\mathbf{8H^+}$ as the sole carbo-

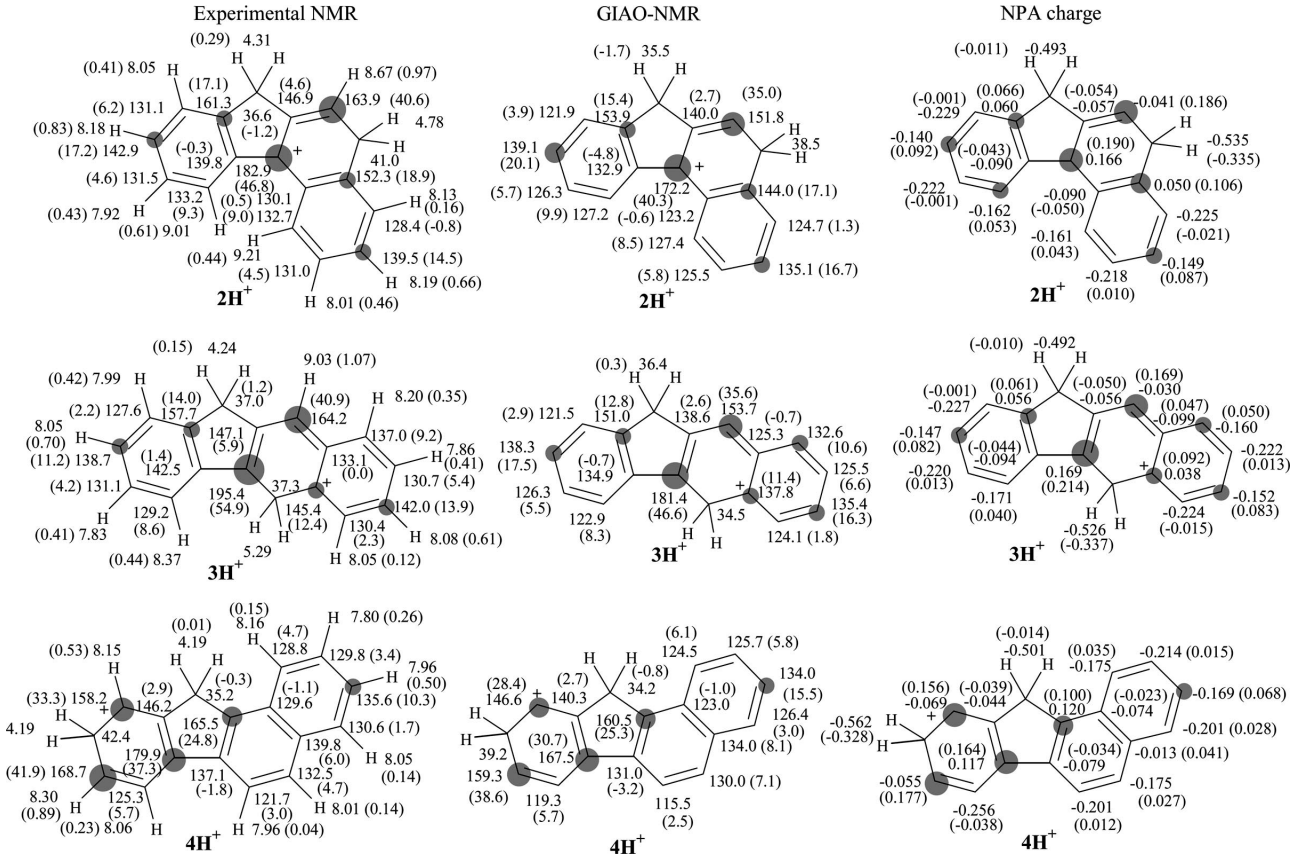

Figure 2. Experimental NMR, GIAO-derived NMR and NPA changes in charges (Δq) for **2H⁺**, **3H⁺** and **4H⁺** [$\Delta\delta^{13}$C, $\Delta\delta^{1}$H, and Δq relative to the corresponding parent compounds in parentheses; dark circles are roughly proportional to the magnitude of $\Delta\delta^{13}$C and Δq (thresholds: 10 and 0.05, respectively)].

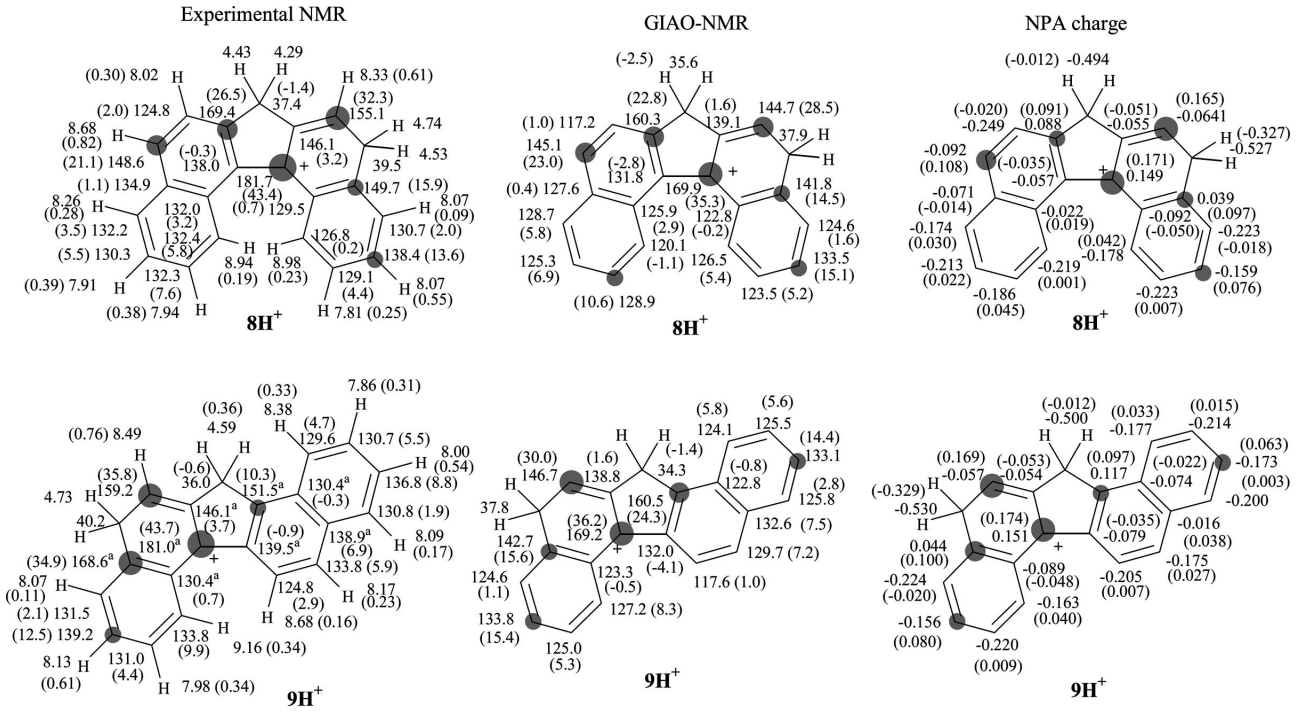

Figure 3. Experimental NMR, GIAO-derived NMR and NPA changes in charges (Δq) for **8H⁺**, and **9H⁺** [$\Delta\delta^{13}$C, $\Delta\delta^{1}$H, and Δq relative to the corresponding parent compounds in parentheses; dark circles are roughly proportional to the magnitude of $\Delta\delta^{13}$C and Δq (thresholds: 10 and 0.05, respectively)].

cation. The charge-delocalization pattern that emerges based on the magnitude of the $\Delta\delta^{13}C$ values from the experiment and from GIAO data (Figure 3) indicates that the positive charge is mainly delocalized within the fluorene moiety, with limited extension into the conjugated carbon atoms in the benzannulated rings.

Protonation of 13*H*-dibenzo[*a*,*g*]fluorene (**9**) with FSO_3H/SO_2ClF resulted in the clean formation of $\mathbf{9H^+}$ as the sole carbocation by protonation at C-11, which is in accord with the DFT-derived relative carbocation energy sequence C-11 >> C-1 > C-3 (Table S1). From the experimental $\Delta\delta^{13}C$ values and GIAO-NMR data (Figure 3), it can be surmised that this carbocation has a relatively short delocalization path, with the positive charge localized mainly in the protonated ring plus two other conjugated carbon atoms.

Quenching of the superacid solutions of the carbocations returned the skeletally intact PAHs in every case (NMR assay).

Comparative Nitration of 11*H*-Benzo[*b*]fluorene (3) and 7*H*-Dibenzo[*c*,*g*]fluorene (8)

See Scheme 2. In order to compare the protonation regioselectivity with the nitration, protic nitrations of **3** and **8** were studied as representative cases (Scheme 2). Thus, mild protic nitration of **3** resulted in the formation of $\mathbf{3NO_2}$ (nitration at C-5) along with two isomeric dinitro derivatives $\mathbf{3a(NO_2)_2}$ and $\mathbf{3b(NO_2)_2}$ in a 2:1:1 ratio. Nitration of **8** occurred selectively at C-5 leading to $\mathbf{8NO_2}$.

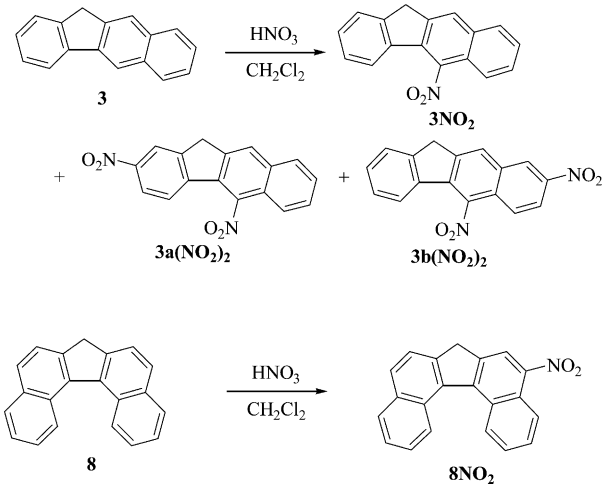

Scheme 2. Nitration of **3** and **8**.

Collectively, the data indicate common regioselectivities in the stable-ion protonation and nitration, which are also in full agreement with relative carbocation energies computed by DFT.

Stable-Ion Study of Methoxy-Substituted 11*H*-Benzo[*a*]fluorenes 5–7 and 13*H*-Dibenzo[*a*,*g*]fluorene (10)

See Scheme 3, Figures 4 and 5, and Table S1. Low-temperature reaction of the 2-methoxy derivative **5** with FSO_3H/SO_2ClF resulted in the protonation at C-1, generating carboxonium ions $\mathbf{5H^+/5aH^+}$ as geometrical isomers in

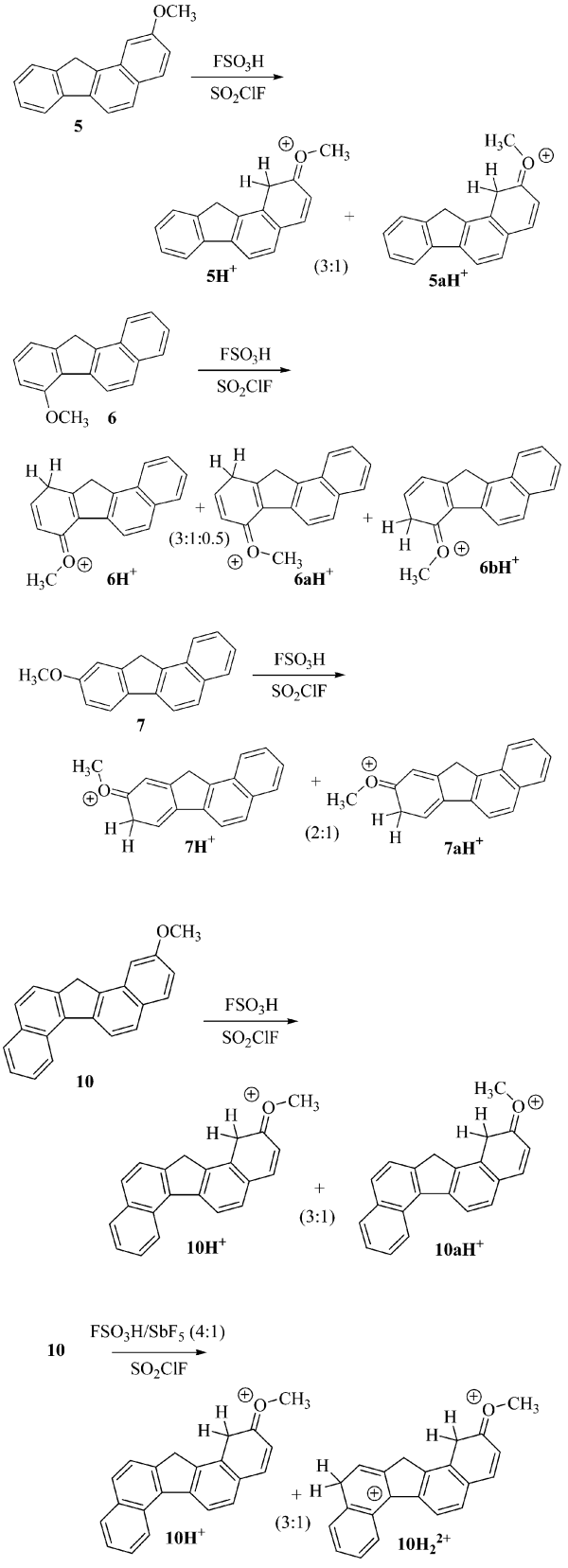

Scheme 3. Stable-ion study of methoxy-substituted 11*H*-benzo[*a*]fluorenes **5**–**7** and 13*H*-dibenzo[*a*,*g*]fluorene (**10**).

a 3:1 ratio. Relative assignment of the carboxonium ions was secured by NOE. As mentioned earlier, the DFT-derived positional reactivity order C-9 > C-1 > C-3 = C-7 was derived for parent **4**, with the arenium ion of protonation at C-1 being only 1 kcal/mol less stable. Protonation of **5** at C-1 appears most logical, as it benefits from both substituent-effect stability and arenium ion stability. The positive charge in the carboxonium ions **5H$^+$/5aH$^+$** is strongly localized in the substituted ring (*ortho*/*para*) and one other conjugated carbon atom (Figure 4).

The 7-methoxy derivative **6** reacted with FSO_3H/SO_2ClF at low temperature to give mainly the carboxonium ions **6H$^+$/6aH$^+$** (in a 3:1 ratio) as geometrical isomers, by attack at C-10 (*para* to methoxy), along with the isomeric carboxonium ion **6bH$^+$** and/or **6cH$^+$** by protonation at C-8 (*ortho*) as minor species.

Whereas protonation at C-10 in parent **4** is unfavorable based on DFT, significant stabilization is gained through the *p*-MeO substituent. Experimental and GIAO-NMR spectroscopic data for **6H$^+$** (major carbocation observed)

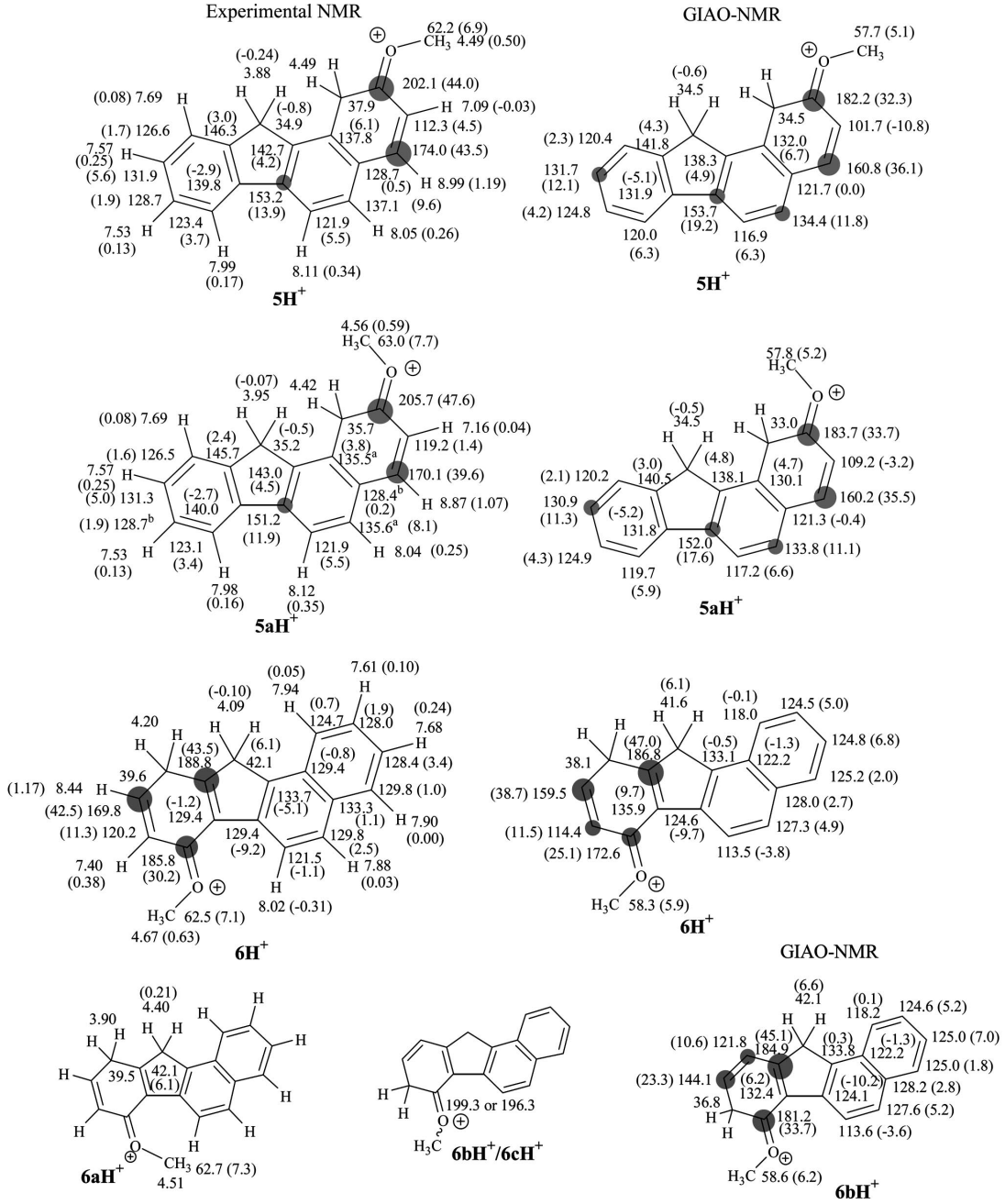

Figure 4. Experimental NMR and GIAO-derived NMR spectroscopic data for carbocations derived from **5** and **6** ($\Delta\delta^1$H and $\Delta\delta^{13}$C relative to the corresponding parent compounds in parentheses; a and b denote interchangeable assignments; nd = not detected; for minor carbocations partial assignments are given, showing only diagnostic signals; dark circles are roughly proportional to the magnitude of $\Delta\delta^{13}$C values; threshold = 10 ppm).

demonstrate that the positive charge is mostly retained in the substituted ring (residing *ortho*/*para* to MeO group).

The complexity of the NMR spectra (mixture of carbocations and large number of overlapping signals) allowed only partial assignments for the minor species. Irradiation of the methyl group of **6H$^+$** led to enhancement of the 8-H signal, along with a smaller enhancement of the 6-H signal. The CH_2 group (protonated site) in **6aH$^+$** was observed as a doublet, which – based on an H/H COSY spectrum – is coupled to 9-H (9-H is coupled to 10-H). According to DFT (Table S1), **6H$^+$** (protonation at C-10) and **6bH$^+$** (protonation at C-8) have very similar energies and are by 8 kcal/mol more stable than **6aH$^+$**and **6cH$^+$** (which also have very similar energies). Based on these data, the presence of **6cH$^+$** as a minor species in the mixture is rather unlikely.

A similar protonation of the 9-methoxy derivative **7** with FSO_3H/SO_2ClF resulted in the formation of the carboxon-

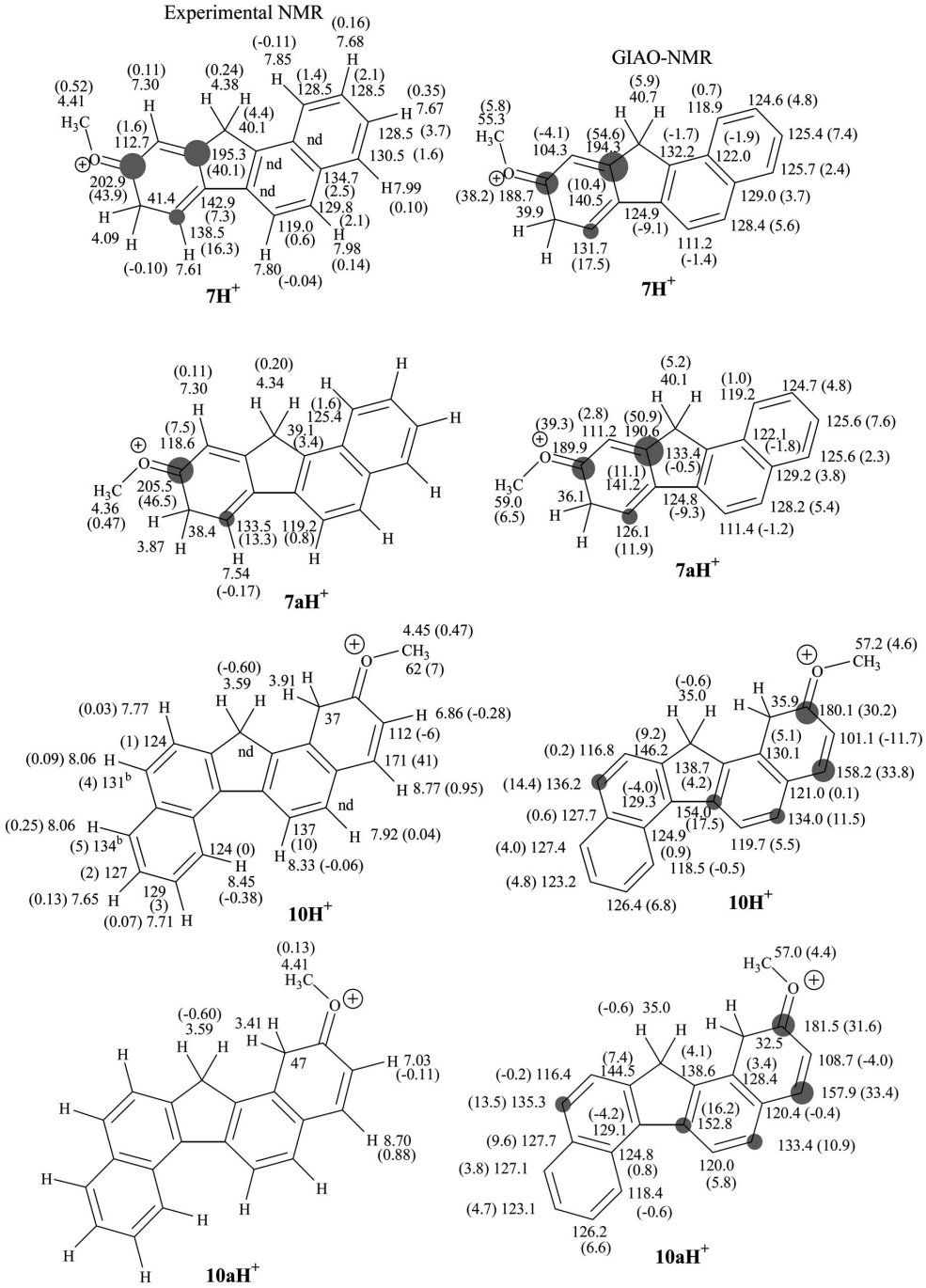

Figure 5. Experimental NMR and GIAO-derived NMR spectroscopic data for carbocations derived from **5** and **6** ($\Delta\delta^1$H and $\Delta\delta^{13}$C relative to the corresponding parent compounds in parentheses; a and b denote interchangeable assignments; nd = not detected; for minor carbocations partial assignments are given, showing only diagnostic signals; dark circles are roughly proportional to the magnitude of $\Delta\delta^{13}$C; the reported diagnostic ^{13}C chemical shifts for **10H$^+$** and **10aH$^+$** are from an HMQC spectrum).

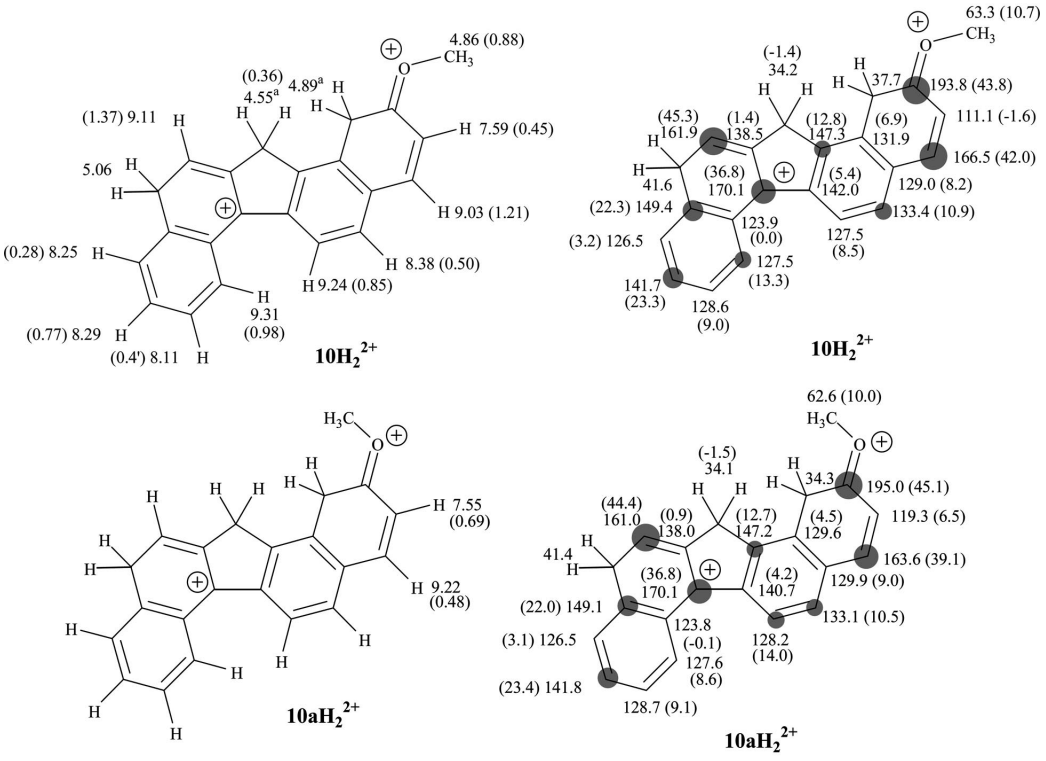

Figure 5. *(Continued)*.

ium ions **7H⁺/7aH⁺** as geometrical isomers by attack at C-8. Analogously to the situation for **6**, although protonation at C-8 is relatively unfavorable in parent **4**, significant stabilization can be gained through the *ortho*-MeO group. The charge delocalization pattern in **7H⁺** is analogous to that in **6H⁺**. The protonation of 2-methoxy-13*H*-dibenzo[*a*,*g*]fluorene (**10**) with FSO_3H/SO_2ClF led to the formation of the carboxonium ions **10H⁺/10aH⁺** as geometrical isomers in a 3:1 ratio. Low-temperature reaction of **10** with FSO_3H/SbF_5 (4:1)/SO_2ClF led to the formation of singly charged **10H⁺** as major species, together with the dications **$10H_2^{2+}$/$10aH_2^{2+}$** as minor species (see Figure 5). Due to the complexity of the NMR spectra (line-broadening and overlapping signals) only partial assignments could be made. The signals of a number of ring-junction carbon atoms in **10H⁺** were undetectable. This problem was remedied with the help of GIAO-NMR, on the basis of which the charge-delocalization pattern for **10H⁺** was deduced (see Figure 5). The carboxonium ion **10H⁺** exhibits a strong naphthalenium ion character, extended into two additional conjugated ring carbon atoms. Quenching of the superacid solutions of the carbocations in all cases returned the skeletally intact precursors.

Comparative Nitration of Methoxy-Substituted 11*H*-Benzo[*b*]fluorenes 5–7 and 13*H*-dibenzo[*a*,*g*]fluorene (10)

See Scheme 4. In order to compare the low-temperature protonation outcome with the nitration in the case of methoxy-substituted derivatives, the benzo[*b*]fluorenes **5**–**7** and

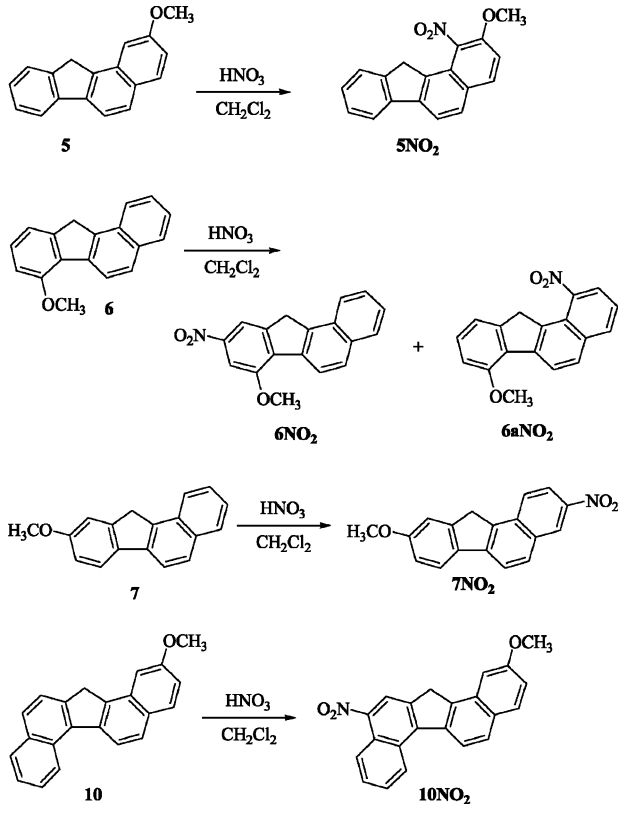

Scheme 4. Nitration of the methoxy-substituted 11*H*-benzo[*a*]fluorenes **5**–**7** and 13*H*-dibenzo[*a*,*g*]fluorene (**10**).

dibenzofluorene **10** were nitrated under very mild conditions (10% HNO_3 in CH_2Cl_2 at 0 °C or room temp.).

Compound **5** (methoxy group at C-2) was efficiently nitrated at C-1 to give **5NO$_2$**, showing therefore a common substituent-driven regiocontrol in the protonation and nitration. The nitration of compound **6** (methoxy group at C-7) gave a 3:1 mixture of two mononitro derivatives **6NO$_2$** and **6aNO$_2$** by substitution at C-9 and C-1, respectively. Considering the DFT-derived relative carbocation stability sequence C-9 > C-1 > C-3 = C-7 and taking into account relatively close energy differences among them (see Table S1), it is conceivable that initial superacid protonation of **6** could have occurred at C-1 and the ion rapidly rearranged to give **6H$^+$**. An alternative scenario, whereby initial protic nitration occurred competitively at C-8/C-10 (*ortho*/*para* to MeO) and the resulting σ complexes subsequently rearranged under equilibrating conditions (at room temp. or 0 °C), cannot be ruled out.

Differing regioselectivities in the protonation and nitration, with regiocontrol of the nitration reflecting the relative σ-complex stability in the parent (unsubstituted) systems, were also observed in the case of **7** (methoxy group at C-9), whose mild protic nitration led to the isolation of **7NO$_2$** by attack at C-3, and in nitration of **10** (methoxy group at C-2), which resulted in a substitution at C-11, forming **10NO$_2$** in high yield, in preference to C-1/C-3.

Stable-Ion Study of the 5,6-Dihydro Derivative 11

See Scheme 5 and Figure 6. Low-temperature reaction of **11** with FSO_3H/SO_2ClF gave a 2:1 mixture of two carbocations, which were identified on the basis of their NMR spectroscopic data as **11H$^+$** and **11aH$^+$**, respectively. Whereas formation of **11aH$^+$** by protonation at C-11 is similar to the protonation outcome in the parent PAH system **9**, *ipso*-protonation at the 5/6 ring junction in the case of **11** is quite novel. A noteworthy feature in the ^{1}H NMR spectrum of **11H$^+$** is the diastereotopic nature of the methylene groups (see Figure 6), whose relative assignments were secured based on NOE measurements. This feature is not

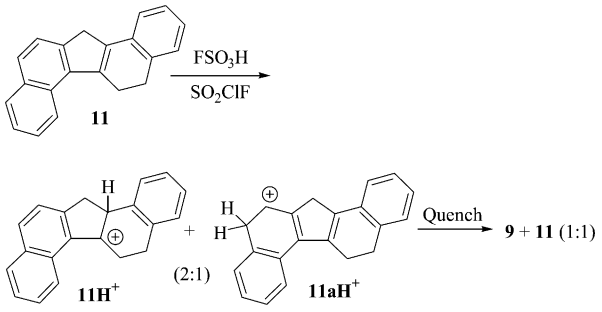

Scheme 5. Stable-ion study of the 5,6-dihydro derivative **11**.

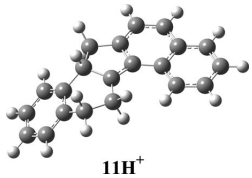

Figure 7. B3LYP/6-31G(d)-optimized structure for **11H$^+$**.

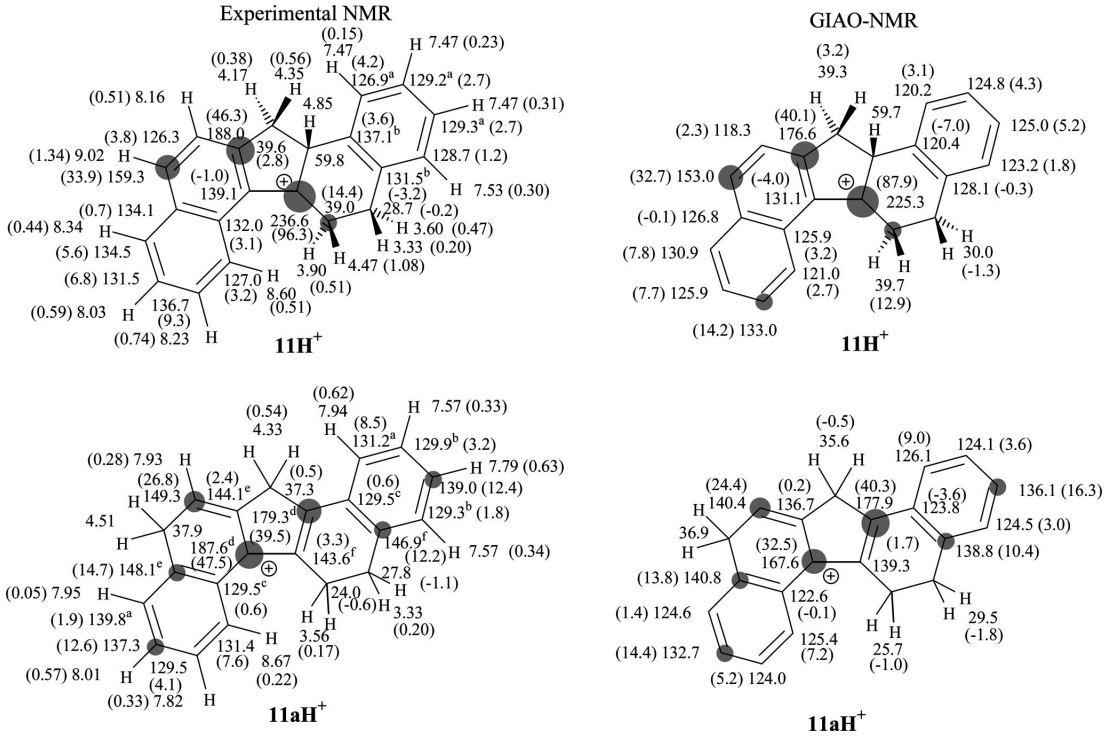

Figure 6. Experimental NMR and GIAO-derived NMR spectroscopic data for various carbocations derived from **11** ($\Delta\delta^1$H and $\Delta\delta^{13}$C relative to the corresponding parent compounds in parentheses; a–f denote interchangeable assignments; dark circles are roughly proportional to the magnitude of $\Delta\delta^{13}$C values).

present in **11aH$^+$**. The DFT-optimized structure of **11H$^+$** is shown in Figure 7. The carbocation has a convex geometry with the methine proton pointing up and the methylene protons pointing up and down. Quenching of the carbocation solution in this case resulted in the formation of a 1:1 mixture of **11/9**.

Mutagenicity Assay on the Nitro Derivatives

The nitro compounds **3NO$_2$**, **5NO$_2$**, **7NO$_2$**, **8NO$_2$** and **10NO$_2$**, which were available in high purity and sufficient quantity, were subjected to a comparative mutagenicity assay by Ames tests, in comparison with their precursors (**3**, **5**, **7**, **8**, and **10**, respectively). The results are summarized in Table 1 (see Experimental Section for the procedure). The precursors themselves were not mutagenic, except for **3** and **10** which were weakly mutagenic with metabolic activation (+S9). In contrast, the nitro derivatives were all mutagenic to some degree. It can be seen (Table 1) that **3NO$_2$** and **5NO$_2$** are weakly mutagenic (with **3NO$_2$** requiring metabolic activation), whereas **7NO$_2$** is strongly mutagenic, especially without S9. Most remarkable are the mutagenic activities of **8NO$_2$** and **10NO$_2$**; **8NO$_2$** is potent with metabolic activation but acts as a potent direct-acting mutagen, producing by far the highest response of all of the compounds tested; **10NO$_2$** is also highly potent but is more active in the presence of S9 mix (with metabolic activation).

Table 1. Mutagenicity assay by Ames tests and nitro group tilt angle from X-ray structures and DFT calculations.

Compound	Potencies (revertants [μg]) of test compounds in TA100 +S9	–S9	Nitro tilt angle [°] X-ray	DFT
3	8.1	NM[a]		
3NO$_2$	15.4	NM[a]	–	57.3
5	NM[a]	NM[a]		
5NO$_2$	25.3	138	89.4	89.7
7	NM[a]	NM[a]		
7NO$_2$	377	13584	–	0.0
8	NM[a]	NM[a]		
8NO$_2$	15828	175107	32.4	27.3
10	1360	NM[a]		
10NO$_2$	28217	5355	–	0.0

[a] NM = not mutagenic; +S9 = with metabolic activation; –S9 = without metabolic activation.

X-ray Structures of the Nitro Derivatives

Metabolism of nitro-PAHs has been studied extensively, and it has been shown that nitro reduction and diol epoxide formation are both important in DNA binding.[11]

The relationship between the nitro group orientation and the mutagenic potency has previously been examined in a number of systems. It was shown that nitro-PAHs with a buttressed (or perpendicular) nitro group are either inactive or weakly active, but other factors namely reduction potentials, molecular structure, degree of aromaticity, and LUMO energies have also been suggested to be important.[12]

The availability of the nitro derivatives synthesized in the present study provided the opportunity to examine their molecular structures by X-ray analysis. This proved successful for **5NO$_2$** and **8NO$_2$**, from which suitable crystals for X-ray analysis could be grown from toluene and hexane, respectively. The ORTEP plots are shown in Figures 8 and 9.

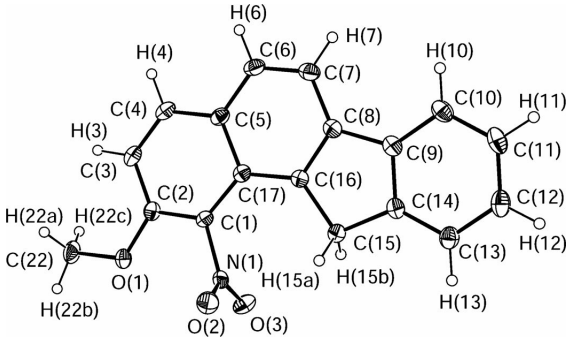

Figure 8. Thermal ellipsoid plot of **5NO$_2$** (ellipsoids are drawn at the 30% level).

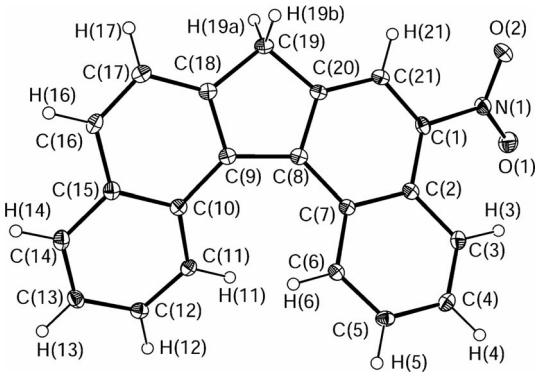

Figure 9. Thermal ellipsoid plot of **8NO$_2$**. Ellipsoids are drawn at the 30% level.

Whereas the MeO group in **5NO$_2$** is almost planar (tilt angle 3°), the nitro group is severely buttressed. The angle between the plane of the nitro group and the plane of the aromatic ring bearing the NO_2 group is 89.4°. In **8NO$_2$** this angle is reduced to 32.4°.

In order to have a larger set for comparing the nitro group tilt angle vs. the mutagenicity, structures of **3NO$_2$**, **5NO$_2$**, **7NO$_2$**, **8NO$_2$** and **10NO$_2$** were optimized by DFT (see Figure S17). The computed nitro tilt angles are incorporated into Table 1 along with the X-ray derived data. It can be seen that the strongly mutagenic compounds are those with coplanar or slightly tilted nitro groups, i.e. **7NO$_2$**, **10NO$_2$** and **8NO$_2$**, whereas weakly mutagenic derivatives are those with severely buttressed nitro groups, namely **5NO$_2$** and **3NO$_2$**. The degree of distortion of the molecular frame in **8NO$_2$** is also noteworthy, with a plane angle between the two outermost rings of 38.5° from the X-ray structure and 34.8° from the DFT calculation. From the optimized structures, in all other cases the periphery is planar. The molecular distortion in **8NO$_2$** could be a contributing factor to its mutagenic activity.[13]

The present findings are in concert with earlier studies on the relationship between mutagenic activity and nitro angle in other classes of nitro-PAHs.[12]

Concluding Remarks and Summary Highlights

In the context of the present study a series of hitherto unknown persistent carbocations and carboxonium ions were generated from benzofluorenes, dibenzofluorenes, and their respective methoxy derivatives, and were studied by NMR spectroscopy and by DFT calculations. Charge-delocalization modes in the resulting species were deduced by NMR and by GIAO-NMR spectroscopic data, and in selected cases were compared with the overall pattern derived based on the computed NPA charges. As the NMR spectroscopic data in the corresponding figures illustrate, there is good overall agreement between the experimentally derived and GIAO-derived charge-delocalization maps, based on $\Delta\delta^{13}$C values. The GIAO shifts computed by B3LYP/6-31G(d) were typically underestimated by 10–15 ppm as compared to the experimental values. Slightly more deshielded values were computed in representative cases by increasing the basis set to B3LYP/6-311G(d,p) (Figure S20), bringing the computed values closer to the experimental data, but the overall pattern of charge delocalization based on $\Delta\delta^{13}$C values remained unchanged. Therefore, the GIAO shifts derived by B3LYP/6-31G(d) were deemed adequate for comparative purposes as a way to derive and compare charge-delocalization modes.

Relative ^{13}C chemical shifts, computed by GIAO-NMR for a given carbocation, were used as model for upgrading the experimental NMR assignments, by reducing the number of interchangeable assignments in complex cases, and as a way to obtain more complete NMR spectroscopic data for the minor carbocations formed in some cases, for which only partial experimental NMR spectroscopic data could be derived.

In view of the environmental significance of nitro-PAHs, nitration was used as model, and several nitro derivatives were synthesized and isolated. Regioselectivity and substituent-effect issues were addressed in comparing nitration, protonation, and DFT data (relative arenium ion energies). Structure/activity relationships in the nitro derivatives were studied by a combined comparative mutagenicity assay (for five compounds), X-ray analysis (in two cases), and structure optimizations. Taken together, the results demonstrate the relationship between nitro buttressing and bioactivity and reinforce the earlier findings in other classes of PAHs, that the highly mutagenic nitro derivatives are those with planar nitro groups, with the severely distorted analogues being inactive.

Experimental Section

General: Melting points are uncorrected. NMR spectra were recorded with a 500-MHz NMR instrument. Electrospray MS (ES-MS) data were obtained in infusion mode by mixing a dilute CH_2Cl_2 solution of compounds with AgOTf in MeOH to form PAH/Ag^+ adducts.[14] IR spectra were obtained with an FT-IR instrument.

Benzofluorenes, Dibenzofluorenes, and Dihydrodibenzofluorene: 11*H*-benzo[*b*]fluorene (**3**) was purchased. 11*H*-Benzo[*a*]fluorene (**4**),[15] 2-methoxy-11*H*-benzo[*a*]fluorene (**5**), 7-methoxy-11*H*-benzo[*a*]fluorene (**6**),[16] 9-methoxy-11*H*-benzo[*a*]fluorene (**7**),[16] 2-methoxy-13*H*-dibenzo[*a*,*g*]fluorene (**10**),[15,18] and 5,6-dihydro-13*H*-dibenzo[*a*,*g*]fluorene (**11**)[18] were available from previous studies by one of us (B. K. B.). 7*H*-Dibenzo[*c*,*g*]fluorene (**8**) was prepared according to a literature procedure.[17] Samples of 7*H*-benzo[*c*]fluorene (**2**)[19] and 13*H*-dibenzo[*a*,*g*]fluorene (**9**)[19] were a gift from Prof. Ronald Harvey (Univ. of Chicago).

Typical Procedure for Stable-Carbocation Generation: A 5-mm NMR tube was charged with the substrate (3–5 mg) and cooled to dry ice/acetone temperature. SO_2ClF (ca. 0.3 mL) was condensed directly into the tube, and a few drops of CD_2Cl_2 were added into the solution. Then a few drops of FSO_3H or FSO_3H/SbF_5 (4:1) were carefully introduced to prevent local overheating, whereupon immediate color changes took place (variable from compound to compound). The NMR sample was vigorously stirred at –78 °C (vortex), to give a homogeneous solution. Reaction of **2** with FSO_3H/SO_2ClF gave a yellow-green solution, whereas all other substrates produced dark-red solutions. Compounds **3**, **8**, and **10** with FSO_3H/SbF_5 (4:1)/SO_2ClF gave dark-red (for **3**) and dark-purple solutions (for **8** and **10**).

Quenching Procedure: The superacid solution was carefully poured into a cold aqueous solution of sodium hydrogen carbonate, and extracted three times with dichloromethane. The combined organic extracts were dried with magnesium sulfate, filtered, and concentrated under reduced pressure. The resulting solid residue was found to be intact starting materials by ^{1}H NMR spectroscopy, except for **11** which gave a 1:1 mixture of **9/11**.

Computational Protocols: Structures were optimized by the density function theory (DFT) method at the B3LYP/6-31G(d) level using the Gaussian 03 package.[20,21] All computed geometries were verified by frequency calculations to have no imaginary frequencies. Energies of the optimized structures for parent systems and their protonation cations are summarized in Table S1 in the Supporting Information. NMR chemical shifts were calculated by the GIAO[22] method at the B3LYP/6-31G(d) level. For comparison, in representative cases, the GIAO shifts were computed at the B3LYP/6-311G(d,p) level, following geometry optimization by B3LYP/6-31G(d). GIAO-NMR chemical shifts were referenced to TMS [GIAO magnetic shielding tensor at δ = 189.8 and 184.7 ppm by B3LYP/6-31G(d) and by B3LYP/6-311G(d,p), respectively; these values are related to the GIAO isotropic magnetic susceptibility for ^{13}C, calculated with molecular symmetry of T_d at the same level of theory].

Nitration Reactions

Nitration of **3** (10.1 mg) with 10% HNO_3 (0.27 g) in CH_2Cl_2 (0.55 g) at room temp. for 3 min gave a mixture of **3NO$_2$**, **3a(NO$_2$)$_2$**, and **3b(NO$_2$)$_2$** as yellow solids. The crude product mixture was purified by SiO_2 column chromatography using hexane/CH_2Cl_2 (1:1) to afford **3NO$_2$** as yellow crystals (5.2 mg, 43%, R_f = 0.68 in hexane/CH_2Cl_2, 1:1) and an isomeric mixture of **3a(NO$_2$)$_2$** and **3b(NO$_2$)$_2$** as yellow crystals (3.1 mg, 22%, R_f = 0.29 in hexane/CH_2Cl_2, 1:1). IR (KBr) for **3a(NO$_2$)$_2$** and **3b(NO$_2$)$_2$**: $\tilde{\nu}\tilde{\nu}$ = 1518, 1340 cm^{-1}. ES-MS (+) for **3a(NO$_2$)$_2$** and **3b(NO$_2$)$_2$**: *m*/*z* = 412.8/414.6 [M + Ag]$^+$. MS/MS = 412.8/414.6 → 300.4.

3NO$_2$: Yellow crystals; m.p. 192.0–194.0 °C. IR (KBr): $\tilde{\nu}$ = 1518, 1408, 1372, 1263, 756, 716 cm^{-1}. ^{1}H NMR (500 MHz, $CDCl_3$): δ =

8.01 (s, 1 H), 7.92 (d, J = 7.5 Hz, 1 H), 7.83 (d, J = 7.5 Hz, 1 H), 7.73 (d, J = 7.5 Hz, 1 H), 7.62 (t, J = 7.5 Hz, 1 H), 7.61 (d, J = 7.5 Hz, 1 H), 7.57 (t, J = 7.5 Hz, 1 H), 7.45 (t, J = 7.5 Hz, 1 H), 7.42 (t, J = 7.5 Hz, 1 H), 4.13 (s, 2 H) ppm. ^{13}C NMR (125 MHz, $CDCl_3$): δ = 144.5 (C), 141.3 (C), 141.1 (C), 136.0 (C), 132.8 (C), 130.7 (C), 129.4 (CH), 127.9 (2 CH), 127.7 (CH), 126.9 (CH), 125.9 (CH), 125.4 (CH), 124.1 (C), 122.9 (CH), 121.4 (CH), 36.1 (CH_2) ppm. ES-MS (+): m/z = 367.8/369.6 $[M + Ag]^+$, 628.4/630.4 $[2 M + Ag]^+$. MS/MS: 367.8/369.6 → 321.5/323.5, 230.3, 105.9, 107.9.

3a(NO$_2$)$_2$: ^{1}H NMR (500 MHz, $CDCl_3$): δ = 8.45 (br. s, 1 H), 8.31 (dd, J = 9.0, 2.0 Hz, 1 H), 8.17 (s, 1 H), 7.97 (d, J = 9.0 Hz, 1 H), 7.86 (d, J = 8.0 Hz, 1 H), 7.82 (d, J = 8.5 Hz, 1 H), 7.69 (m, 1 H), 7.66 (m, 1 H), 4.26 (s, 2 H) ppm. ^{13}C NMR: δ = 148.0 (C), 145.5 (C), 142.1 (C), 141.2 (C), 133.7 (C), 128.6 (CH), 128.3 (C), 128.1 (CH), 128.1 (CH), 126.5 (CH), 124.0 (C), 123.5 (CH), 123.3 (CH), 121.8 (CH), 120.5 (CH), 36.2 (CH_2) ppm.

3b(NO$_2$)$_2$: ^{1}H NMR (500 MHz, $CDCl_3$): δ = 8.86 (d, J = 2.0 Hz, 1 H), 8.37 (dd, J = 9.0, 2.0 Hz, 1 H), 8.26 (s, 1 H), 7.95 (d, J = 9.0 Hz, 1 H), 7.75 (d, J = 7.5 Hz, 1 H), 7.65 (m, 1 H), 7.53 (t, J = 7.5 Hz, 1 H), 7.47 (t, J = 7.5 Hz, 1 H), 4.19 (s, 2 H) ppm. ^{13}C NMR: δ = 145.8 (C), 145.0 (C), 144.0 (C), 135.1 (C), 134.6 (C), 131.3 (C), 130.8 (CH), 128.1 (CH), 127.6 (CH), 126.6 (C), 125.6 (CH), 124.4 (CH), 123.5 (CH), 123.3 (CH), 121.3 (CH), 36.2 (CH_2) ppm.

Nitration of **5** (11 mg) in 10% HNO_3/CH_2Cl_2 at 0 °C for 5 min gave a yellow oil, which after purification by SiO_2 column chromatography using hexane/CH_2Cl_2 (1:1) afforded **5NO$_2$** as yellow crystals (12 mg, 89% yield, R_f = 0.50 in hexane/CH_2Cl_2, 1:1).

5NO$_2$: Yellow crystals; m.p. 155.0–157.0 °C. IR (KBr): $\tilde{\nu}$ = 1631, 1528, 1277, 1100, 825, 758 cm^{-1}. ^{1}H NMR (500 MHz, $CDCl_3$): δ = 7.97 (d, J = 9.0 Hz, 1 H), 7.88 (d, J = 8.5 Hz, 1 H), 7.85 (d, J = 8.5 Hz, 1 H), 7.82 (d, J = 7.5 Hz, 1 H), 7.56 (d, J = 7.5 Hz, 1 H), 7.40 (t, J = 7.5 Hz, 1 H), 7.35 (t, J = 7.5 Hz, 1 H), 7.26 (d, J = 9.0 Hz, 1 H), 4.05 (s, 2 H), 4.03 (s, 3 H) ppm. ^{13}C NMR (125 MHz, $CDCl_3$): δ = 149.3 (C), 143.7 (C), 142.7 (C), 140.7 (C), 135.1 (C), 133.4 (C), 132.6 (CH), 128.4 (CH), 128.1 (C), 127.4 (CH), 126.8 (CH), 124.7 (CH), 122.8 (C), 119.9 (CH), 118.2 (CH), 111.6 (CH), 57.0 (CH_3), 34.8 (CH_2) ppm. ES-MS (+): m/z = 398.0/400.0 $[M + Ag]^+$, 688.8/690.8 $[2 M + Ag]^+$. MS/MS: 398.0/400.0 → 352.1/354.1, 274.2, 261.2.

Nitration of **6** (7.5 mg) in 10% HNO_3/CH_2Cl_2 at 0 °C for 5 min gave **6**, **6NO$_2$**, **6aNO$_2$**, together with small amounts of other compounds (yellow crystals), which after purification by SiO_2 column chromatography using hexane/CH_2Cl_2 (1:1) afforded mainly **6NO$_2$** as yellow crystals (5.4 mg, 61% yield, R_f = 0.31 in hexane/CH_2Cl_2, 1:1) and **6aNO$_2$** as a brown powder (2.0 mg, 20% yield, R_f = 0.56 in hexane/CH_2Cl_2, 1:1).

6NO$_2$: IR (KBr): $\tilde{\nu}$ = 1522, 1505, 1330, 1092, 817, 740 cm^{-1}. ^{1}H NMR (500 MHz, $CDCl_3$): δ = 8.32 (d, J = 8.0 Hz, 1 H), 8.11 (br. s, 1 H), 7.99 (d, J = 8.0 Hz, 1 H), 7.93 (d, J = 8.0 Hz, 1 H), 7.89 (d, J = 8.0 Hz, 1 H), 7.80 (br. s, 1 H), 7.57 (t, J = 8.0 Hz, 1 H), 7.52 (t, J = 8.0 Hz, 1 H), 4.23 (s, 2 H), 4.11 (s, 3 H) ppm. ^{13}C NMR (125 MHz, $CDCl_3$): δ = 155.0 (C), 147.1 (C), 145.0 (C), 141.7 (C), 137.2 (C), 136.6 (C), 133.0 (C), 129.9 (C), 128.9 (CH), 128.1 (CH), 126.7 (CH), 126.3 (CH), 124.2 (CH), 122.6 (CH), 113.2 (CH), 105.0 (CH), 56.0 (CH_3), 36.3 (CH_2) ppm. ES-MS (+): m/z = 397.6/399.5 $[M + Ag]^+$, 688.3/690.3 $[2 M + Ag]^+$. MS/MS: 397.6/399.5 → 290.4, 273.3.

6aNO$_2$: IR (KBr): $\tilde{\nu}$ = 1509, 1263, 1077 cm^{-1}. ^{1}H NMR (500 MHz, $CDCl_3$): δ = 8.54 (d, J = 8.5 Hz, 1 H), 8.08 (d, J = 8.5 Hz, 1 H), 7.96 (d, J = 9.0 Hz, 1 H), 7.68 (d, J = 7.0 Hz, 1 H), 7.44 (t, J = 8.0 Hz, 1 H), 7.33 (t, J = 8.0 Hz, 1 H), 7.20 (d, J = 7.0 Hz, 1 H), 6.93 (d, J = 8.0 Hz, 1 H), 4.10 (s, 2 H), 4.05 (s, 3 H) ppm. ^{13}C NMR (125 MHz, $CDCl_3$): δ = 155.9 (C), 145.7 (C), 143.8 (C), 142.7 (C), 134.1 (C), 133.1 (C), 132.9 (CH), 129.1 (C), 128.6 (CH), 128.3 (CH), 124.6 (CH), 122.9 (CH), 121.5 (CH), 117.1 (CH), 108.8 (CH), 55.4 (CH_3), 36.5 (CH_2) ppm. ES-MS (+): m/z = 397.4/399.4 $[M + Ag]^+$, 688.3/690.3 $[2 M + Ag]^+$. MS/MS: 397.6/399.5 → 290.0, 273.3, 260.3.

Nitration of **7** (7.7 mg) in 10% HNO_3/CH_2Cl_2 at 0 °C for 5 min gave unreacted **7** and **7NO$_2$** as a yellow solid. Purification by SiO_2 column chromatography using hexane/CH_2Cl_2 (1:1) afforded **7NO$_2$** as yellow crystals (3.0 mg, 33% yield, R_f = 0.25 in hexane/CH_2Cl_2, 1:1).

7NO$_2$: Yellow crystals; m.p. 261.0–263.0 °C. IR (KBr): $\tilde{\nu}$ = 1618, 1508, 1331 cm^{-1}. ^{1}H NMR (500 MHz, $CDCl_3$): δ = 8.85 (d, J = 2.0 Hz, 1 H), 8.28 (dd, J = 9.0, 2.0 Hz, 1 H), 8.04 (d, J = 9.0 Hz, 1 H), 8.03 (d, J = 8.0 Hz, 1 H), 7.98 (d, J = 8.0 Hz, 1 H), 7.78 (d, J = 8.5 Hz, 1 H), 7.23 (br. s, 1 H), 7.01 (dd, J = 8.5, 2.5 Hz, 1 H), 4.19 (s, 2 H), 3.92 (s, 3 H) ppm. ^{13}C NMR (125 MHz, $CDCl_3$): δ = 160.1 (C), 145.7 (C), 144.5 (C), 143.1 (C), 138.6 (C), 134.6 (C), 133.1 (C), 130.5 (C), 130.1 (CH), 125.9 (CH), 125.2 (CH), 121.2 (CH), 120.5 (CH), 120.0 (CH), 113.2 (CH), 110.9 (CH), 55.6 (CH_3), 35.7 (CH_2) ppm. ES-MS (+): m/z = 397.6/399.5 $[M + Ag]^+$, 688.2/690.2 $[2 M + Ag]^+$. MS/MS: 397.6/399.5 → 290.2.

Nitration of **8** (5.8 mg) in 25% HNO_3/CH_2Cl_2 at 0 °C for 5 min gave **8** and **8NO$_2$** as a brown oil. Purification by SiO_2 column chromatography using hexane/CH_2Cl_2 (1:1) afforded **8NO$_2$** as brown crystals (3.3 mg, 49% yield, R_f = 0.26 in hexane/CH_2Cl_2, 1:1).

8NO$_2$: Yellow crystals; m.p. 215.0–217.0 °C. IR (KBr): $\tilde{\nu}$ = 1509, 1499, 1327, 1121, 1100 cm^{-1}. ^{1}H NMR (500 MHz, $CDCl_3$): δ = 8.81 (d, J = 8.5 Hz, 1 H), 8.74 (d, J = 8.5 Hz, 1 H), 8.63 (d, J = 8.0 Hz, 1 H), 8.53 (s, 1 H), 8.00 (d, J = 7.5 Hz, 1 H), 8.03 (d, J = 8.0 Hz, 1 H), 7.79 (d, J = 8.0 Hz, 1 H), 7.76 (t, J = 8.0 Hz, 1 H), 7.66 (t, J = 8.0 Hz, 1 H), 7.61 (t, J = 8.0 Hz, 1 H), 7.58 (t, J = 8.0 Hz, 1 H), 4.21 (s, 2 H) ppm. ^{13}C NMR (125 MHz, $CDCl_3$): δ = 145.5 (C), 145.1 (C), 144.8 (C), 140.0 (C), 136.5 (C), 133.9 (C), 130.0 (CH), 129.1 (CH), 128.9 (2 C), 128.4 (CH), 127.0 (CH), 126.1 (CH), 126.0 (C), 125.7 (2 CH), 125.6 (CH), 123.8 (CH), 122.8 (CH), 121.0 (CH), 38.7 (CH_2) ppm. ES-MS (+): m/z = 417.4/419.4 $[M + Ag]^+$, 728.3/730.2 $[2 M + Ag]^+$. MS/MS: 417.4/419.4 → 310.4.

Nitration of **10** (1.8 mg) in 25% HNO_3/CH_2Cl_2 at 0 °C for 5 min gave a brown solid which was purified by SiO_2 column chromatography using hexane/CH_2Cl_2 (1:1) to give **10NO$_2$** as brown crystals (1.9 mg, 90% yield, R_f = 0.12 in hexane/CH_2Cl_2, 1:1).

10NO$_2$: M.p. 235.0–237.0 °C. IR (KBr): $\tilde{\nu}$ = 1627, 1500, 1313, 1228, 821 cm^{-1}. ^{1}H NMR (500 MHz, $CDCl_3$): δ = 8.98 (d, J = 9.5 Hz, 1 H), 8.71 (d, J = 9.5 Hz, 1 H), 8.50 (s, 1 H), 8.42 (d, J = 8.5 Hz, 1 H), 7.94 (d, J = 8.5 Hz, 1 H), 7.87 (d, J = 8.5 Hz, 1 H), 7.78–7.74 (m, 2 H), 7.29 (d, J = 2.0 Hz, 1 H), 7.22 (d, J = 9.0, 2.0 Hz, 1 H), 4.28 (s, 2 H), 4.01 (s, 3 H) ppm. ^{13}C NMR (125 MHz, $CDCl_3$): δ = 158.6 (C), 145.0 (C), 143.7 (C), 142.4 (C), 139.6 (C), 138.8 (C), 131.3 (C), 130.3 (CH), 129.9 (C), 128.3 (CH), 128.2 (CH), 128.1 (C), 125.6 (C), 124.3 (CH), 124.2 (CH), 121.3 (CH), 119.5 (CH), 119.4 (CH), 102.4 (CH), 55.5 (CH_3), 36.6 (CH_2) ppm. ES-MS (+): m/z = 447.5/449.5 $[M + Ag]^+$, 788.5/790.5 $[2 M + Ag]^+$. MS/MS: 447.5/449.5 → 340.5.

Specific NMR assignments for the synthesized nitro-PAHs were assisted by various 2D and 1D techniques (HMQC, HMBC, COSY, and NOE) and are summarized in Figure S2.

Mutagenicity Assays by Ames Tests

Materials: Sodium azide, 2-anthramine (2-aminoanthracene), Aroclor 1254 induced Sprague–Dawley rat liver S9, and DMSO (all from commercial sources).

Procedure: Stock solutions of each compound were prepared at 2 mg/mL in DMSO and maintained at –20 °C. The mutagenic potencies of the compounds were determined in the *Salmonella* mutagenicity assay, using the standard plate-incorporation assay.[23] The compounds were tested in TA100 [*hisG46, rfa-1001, chl-1005 (bio uvrB gal) pKM101*] (provided by Dr. B. N. Ames, University of California, Children's Hospital Oakland Research Institute, Oakland, CA); all compounds were tested in the presence and absence of S9. DMSO was used as a negative control; 2-anthramine was the positive control with S9, and sodium azide was the positive control without S9. Each compound was tested in 2 or 3 independent assays at 1 or 2 plates per dose (each compound with demonstrated mutagenicity was tested at least once at 2 plates per dose). Three plates were used for all DMSO controls. Each compound was tested at an initial dose range of 2–80 μg/plate, and doses were adjusted in the replicate experiments to define the linear dose ranges for each compound. The plates were incubated at 37 °C for 3 d and counted with an AccuCount 1000 automated colony counter. Potencies are reported as revertants (rev)/μg.

General X-ray Crystal Structure Information: X-ray crystallography was performed by mounting a crystal onto a thin glass fiber from a pool of Fluorolube™ and immediately placing it under a liquid N_2 stream on an X-ray diffractometer. The radiation used was graphite-monochromatized Mo-K_α radiation (λ = 0.7107 Å). The lattice parameters were optimized from a least-squares calculation on carefully centered reflections. Lattice determination, data collection, structure refinement, scaling, and data reduction were carried out using the APEX2 version 1.0-27 software package. Data-collection parameters are given in Table S2. Each structure was solved by direct methods. This procedure yielded a number of the C, N, and O atoms. Subsequent Fourier synthesis yielded the remaining atom positions. The hydrogen atoms were fixed in positions of ideal geometry and refined within the XSHELL software. These idealized hydrogen atoms had their isotropic temperature factors fixed at 1.2 or 1.5 times the equivalent isotropic U of the C atoms to which they are bonded. The final refinement of each compound included anisotropic thermal parameters on all non-hydrogen atoms. Additional information concerning the data collection and final structural solutions of compounds **5NO$_2$** and **8NO$_2$** can be found in the Supporting Information. CCDC-658236 (**5NO$_2$**) and -658235 (**8NO$_2$**) contain the supplementary crystallographic data for this paper. These data can be obtained free of charge from The Cambridge Crystallographic Data Centre via www.ccdc.cam.ac.uk/data_request/cif.

Supporting Information (see footnote on the first page of this article): NMR assignments for the neutrals, GIAO-derived ^{13}C NMR chemical shifts with higher basis set, NMR spectra for the nitro derivatives and carbocations, energies for the optimized structures of the carbocations and optimized geometries for the nitro derivatives.

Acknowledgments

Support of this study under "Reactive Intermediates of Carcinogenesis of PAHs" at KSU by the National Cancer Institute of National Institutes of Health (2R15-CA078235-02A1) is gratefully acknowledged. B. K. B. thanks the National Institutes of Health – SCORE for support (2S06M008038-36). We also thank Prof. Ronald Harvey (Ben May Institute, University of Chicago) for samples of 7*H*-benzo[*c*]fluorene (**2**) and 13*H*-dibenzo[*a*,*g*]fluorene (**9**).

[1] A. Koganti, R. Singh, K. Rozett, N. Modi, L. S. Goldstein, T. A. Roy, F. Zhang, R. G. Harvey, E. H. Weyand, *Carcinogenesis* **2000**, *21*, 1601–1609.
[2] E. H. Weyand, B. Parimoo, K. R. Reuhl, L. S. Goldtsein, J. Q. Wang, R. G. Harvey, *Polycyclic Aromat. Compd.* **2004**, *24*, 1–20.
[3] J.-Q. Wang, E. H. Weyand, R. G. Harvey, *J. Org. Chem.* **2002**, *67*, 6216–6219.
[4] B. K. Banik, C. Mukhopadhyay, F. F. Becker, *Synth. Commun.* **2001**, *31*, 2399–2403.
[5] a) B. K. Banik, F. F. Becker, *Curr. Med. Chem.* **2001**, *8*, 1513–1533; b) B. K. Banik, C. Mukhopadhyay, F. F. Becker, *Abstract of 226 ACS National Meeting*, Sept. **2003**.
[6] a) R. Bolton, *J. Chem. Res. (S)* **1977**, *6*, 149; b) K. W. Bair, EP182609, *Chem. Abstr.* **1986**, *105*, 152751; c) E. D. Bergmann, J. Szmuszkovicz, *Bull. Res. Counc. Isr.* **1952**, *1*, 90–92, *Chem. Abstr.* **1953**, *47*, 51492; d) E. D. Bergmann, E. Fischer, Y. Hirshberg, D. Lavie, Y. Sprinzak, J. Szmuszkovicz, *Bull. Soc. Chim. Fr.* **1953**, 798–809.
[7] a) R. G. Harvey, *Polycyclic Aromatic Hydrocarbons*, Wiley-VCH, Weinheim, **1997**, chapter 8; b) R. G. Harvey, *Polycyclic Aromatic Hydrocarbons*, Wiley-VCH, Weinheim, **1997**, chapter 9.
[8] a) S. Samajdar, F. F. Becker, B. K. Banik, *Tetrahedron Lett.* **2000**, *41*, 8017–8020; b) J. W. Cook, R. W. G. Preston, *J. Chem. Soc.* **1944**, 553–561; c) F. F. Becker, C. Mukhopadhyay, L. Hackfeld, I. Banik, B. K. Banik, *Bioorg. Med. Chem.* **2000**, *8*, 2693–2699.
[9] C. L. Ritter, S. J. Culp, J. P. Freeman, M. M. Marques, F. A. Beland, D. Malejka-Giganti, *Chem. Res. Toxicol.* **2002**, *15*, 536–544.
[10] M. Ma, K. E. Johnson, *J. Am. Chem. Soc.* **1995**, *117*, 1508–1513.
[11] See, for example: a) P. P. Fu, Y.-C. Ni, Y.-M. Zhang, R. H. Heflich, Y.-K. Wang, J.-S. Lai, *Mutat. Res.* **1989**, *225*, 121–125; b) S.-T. Lin, Y.-F. Jih, P. P. Fu, *J. Org. Chem.* **1996**, *61*, 5271–5273; c) K. Fukuhara, M. Takei, H. Kageyama, N. Miyata, *Chem. Res. Toxicol.* **1995**, *8*, 47–54; d) N. Sera, K. Fukuhara, N. Miyata, H. Tokiwa, *Mutat. Res.* **1996**, *349*, 137–144.
[12] See, for example: a) P. P. Fu, M. W. Chou, F. A. Beland, in *Polycyclic Aromatic Hydrocarbon Carcinogenesis: Structure-Activity Relationships* (Eds.: S. K. Yang, B. D. Silverman), CRC Press, Boca Raton, Florida, **1988**, vol. 2, chapter 2; P. P. Fu, Y.-C. Ni, Y.-M. Zhang, R. H. Heflich, Y.-K. Wang, J.-S. Lai, *Mutat. Res.* **1989**, *225*, 121–125; b) S.-T. Lin, Y.-F. Jih, P. P. Fu, *J. Org. Chem.* **1996**, *61*, 5271–5273; c) K. Fukuhara, M. Takei, H. Kageyama, N. Miyata, *Chem. Res. Toxicol.* **1995**, *8*, 47–54; d) N. Sera, K. Fukuhara, N. Miyata, H. Tokiwa, *Mutat. Res.* **1996**, *349*, 137–144.
[13] a) A. K. Katz, H. L. Carrell, J. P. Glusker, *Carcinogenesis* **1998**, *19*, 1641–1648; b) C. J. Carrell, H. L. Carrell, J. P. Glusker, E. Abu-Shaqara, C. Cortez, R. G. Harvey, *Carcinogenesis* **1994**, *15*, 2931–2936; c) K. Prout, A. D. Smith, G. H. Daub, D. E. Zacharias, J. P. Glusker, *Carcinogenesis* **1992**, *13*, 1775–1782; d) J. Krzeminski, J.-M. Lin, S. Amin, S. S. Hechet, *Chem. Res. Toxicol.* **1994**, *7*, 125–129.
[14] K. K. Laali, S. Hupertz, A. G. Temu, S. E. Galembeck, *Org. Biomol. Chem.* **2005**, *3*, 2319.
[15] B. K. Banik, M. Cordoba, J. Marquez, *Chemistry (Rajkot, India)* **2006**, *3*, 72–75.
[16] A. Rao, S. Lala, R. R. Rao, *Indian J. Chem., Sect. B Org. Chem. Incl. Med. Chem.* **1984**, *23*, 603–610.
[17] R. Kuhn, D. Rewicki, *Angew. Chem. Int. Ed. Engl.* **1967**, *6*, 635–636; R. H. Martin, *J. Chem. Soc.* **1941**, 679–685.
[18] B. K. Banik, A. Ghatak, C. Mukhopadhyay, F. F. Becker, *J. Chem. Res. (S)* **2000**, 108–109.

[19] R. G. Harvey, J. Pataki, C. Cortez, P. Di Raddo, C. X. Yang, *J. Org. Chem.* **1991**, *56*, 1210–1217.
[20] W. Koch, M. C. Holthausen, *A Chemist's Guide to Density Functional Theory*, 2nd ed., Wiley-VCH, Weinheim, **2000**.
[21] M. J. Frisch, G. W. Trucks, H. B. Schlegel, G. E. Scuseria, M. A. Robb, J. R. Cheeseman, J. A. Montgomery Jr, T. Vreven, K. N. Kudin, J. C. Burant, J. M. Millam, S. S. Iyengar, J. Tomasi, V. Barone, B. Mennucci, M. Cossi, G. Scalmani, N. Rega, G. A. Petersson, H. Nakatsuji, M. Hada, M. Ehara, K. Toyota, R. Fukuda, J. Hasegawa, M. Ishida, T. Nakajima, Y. Honda, O. Kitao, H. Nakai, M. Klene, X. Li, J. E. Knox, H. P. Hratchian, J. B. Cross, C. Adamo, J. Jaramillo, R. Gomperts, R. E. Stratmann, O. Yazyev, A. J. Austin, R. Cammi, C. Pomelli, J. W. Ochterski, P. Y. Ayala, K. Morokuma, G. A. Voth, P. Salvador, J. J. Dannenberg, V. G. Zakrzewski, S. Dapprich, A. D. Daniels, M. C. Strain, O. Farkas, D. K. Malick, A. D. Rabuck, K. Raghavachari, J. B. Foresman, J. V. Ortiz, Q. Cui, A. G. Baboul, S. Clifford, J. Cioslowski, B. B. Stefanov, G. Liu, A. Liashenko, P. Piskorz, I. Komaromi, R. L. Martin, D. J. Fox, T. Keith, M. A. Al-Laham, C. Y. Peng, A. Nanayakkara, M. Challacombe, P. M. W. Gill, B. Johnson, W. Chen, M. W. Wong, C. Gonzalez, J. A. Pople, *Gaussian 03*, Revision B.05, Gaussian, Inc., Pittsburgh, PA, **2003**.
[22] a) K. Wolinski, J. F. Hinton, P. Pulay, *J. Am. Chem. Soc.* **1990**, *112*, 8251–8260; b) R. Ditchfield, *Mol. Phys.* **1974**, *27*, 789–807.
[23] D. M. Maron, B. N. Ames, *Mutat. Res.* **1983**, *113*, 173–215.
Received: November 9, 2007
Published Online: February 12, 2008

